Journal of Power Sources 196 (2011) 4306–4313

Contents lists available at ScienceDirect

Journal of Power Sources

journal homepage: www.elsevier.com/locate/jpowsour

Scale-up of a high temperature polymer electrolyte membrane fuel cell based on polybenzimidazole

F. Javier Pinar, Pablo Cañizares, Manuel A. Rodrigo, Diego Úbeda, Justo Lobato*

Chemical Engineering Department, University of Castilla-La Mancha, Enrique Costa Building, Av. Camilo Jose Cela, n 12, E-13071 Ciudad Real, Spain

ARTICLE INFO

Article history:
Received 19 November 2010
Accepted 23 November 2010
Available online 2 December 2010

Keywords:
PEMFC
Polybenzimidazole
Stack
Dynamic response
Degradation

ABSTRACT

A high temperature PEM fuel cell stack with a total active area 150 cm^2 has been studied. The PEM technology is based on a polybenzimidazole (PBI) membrane. Cast from a PBI polymer synthesised in our lab, the performance of a three-cell stack was analysed in static and dynamic modes. In static mode, operating at high constant oxygen flow rate ($Q_{O_2} > 1105$ ml O_2/min) produces a small decrease on the stack performance. High constant oxygen stoichiometry ($\lambda_{O_2} > 3$) does not produce a decrease on the performance of the stack. There are not differences between operating at constant flow rate of oxygen and constant stoichiometry of oxygen in the stack performance. The effect of operating at high temperature with a pressurization system and operating at higher temperatures are beneficial since the performance of the fuel cell is enhanced. A large shut-down stage produces important performance losses due to the loss of catalyst activity and the loss of membrane conductivity. After 150 h of operation at 0.2 A cm^{-2}, it is observed a very high voltage drop. The phosphoric acid leached from the stack was also evaluated and did not exceed 2% (w/w). This fact suggests that the main degradation mechanism of a fuel cell stack based on polybenzimidazole is not the electrolyte loss. In dynamic test mode, it was observed a rapid response of power and current output even at the lower step-time (10 s). In the static mode at 125 °C and 1 atm, the stack reached a power density peak of 0.29 W cm^{-2} (43.5 W) at 1 V.

1. Introduction

Renewable energy sources and technologies based on hydrogen as an energy carrier, are considered an excellent alternative for generating clean and efficient energy.

From the different types of fuel cells that exist, the most interesting both for stationary and portable applications are polymer electrolyte membrane fuel cells (PEMFCs) due to its high efficiency and zero emission of pollutants [1].

The advantages of polymer electrolyte membrane fuel cells when operating at high temperature (above 100 °C and up to 200 °C) are: (i) increase kinetics for cathode and anode reactions, (ii) greater tolerance of catalyst to impurities and (iii) possibility of using waste heat generated [2]. One of the most promising membranes is polybenzimidazole (PBI) doped with phosphoric acid. Thus, high temperature PEMFC using polybenzimidazole (PBI) doping phosphoric acid membranes as proton conducting electrolyte are available to work at high temperatures and low humidity environment [3–6].

Stability and performance of the high temperature PEMFC are significantly affected by operating conditions such as temperature, flow rates and pressure. In order to achieve a better performance and reach an integration of these systems in power generation applications, several parameters in a fuel cell must be optimized.

The most significant advances in this field reached by this working group have been: (i) development of membranes based on polybenzimidazole (PBI) doped with phosphoric acid [2,7,8], (ii) study of the catalyst ink, optimization of the amount of catalyst and the amount of ionomer in the catalytic layer [9–11] and its subsequent impregnation with the electrolyte to facilitate proton transport and (iii) optimization of the amount of active carbon and Teflon, both on microporous and gas diffusion layers [12,13].

The next step was focused on the assembly and operation of a high temperature PEM stack which is shown in this work. Fuel cell stack development is a key technology for the fuel cell commercialization. Characteristics of the fuel cell stack performance are different from combustion engine and batteries. For an optimal design of the high temperature fuel cell system is required to gain experience previously at a lower scale (pilot plant). Thus, it was studied the influence of temperature and reaction stoichiometry (flow rate of reactants) on the overall performance. Also a durability–stability test was performed on the stack. The durability–stability test was carried out at constant and variable

* Corresponding author. Tel.: +34 926 29 53 00x6707; fax: +34 926 29 52 56.
E-mail address: Justo.Lobato@uclm.es (J. Lobato).

0378-7753/$ – see front matter © 2010 Elsevier B.V. All rights reserved.
doi:10.1016/j.jpowsour.2010.11.137

current using air as comburent in order to simulate a real engine operation. During these experiments the losses of electrolyte contained in both cathode and anode were analysed due to that the loss of electrolyte seems to be one of the main mechanisms of degradation of the PEM fuel cell based on PBI [14]. The electrochemical characterization was performed using cyclic voltammetry measurements for the overall system and for each cell.

2. Experimental

On top of a gas diffusion layer (Toray Graphite Paper, TGPH-120, 350 μm thick, 10% wet-proofing, BASF Fuel Cell, Inc.), a microporous layer (MPL) was deposited by N_2-spraying, consisting of 2 mg cm^{-2} Vulcan XC-72R Carbon Black (Cabot Corp.) and 10% PTFE (Teflon™ Emulsion Solution, Electrochem Inc.). Then, a catalyst layer was also deposited by N_2-spraying, composed of Pt/C catalyst (40% Pt on Vulcan XC-72R Carbon Black, ETEK-Inc.), PBI ionomer (1.24 wt.% PBI in N,N-dimethylacetamide, DMAc) and DMAc as solvent. In all cases, the platinum loading on both electrodes was 0.4 mg Pt cm^{-2}, a C/PBI weight ratio of 20 was used, electrode area was 50 cm^2, and both carbon on microporous layer and platinum on catalyst layer loadings were controlled by the electrode weight increase. Once deposited all the layers, the electrodes were dried at 190 °C for 2 h. Afterwards, the electrodes were wetted with a solution of 1% H_3PO_4, and left to absorb the acid for 1 day.

For the preparation of the MEA (membrane-electrode assembly), a PBI membrane was taken out from a 75 wt.% phosphoric acid bath. Doping level acquired by the membrane was 6.6 molecules of acid per polymer repeating unit. The superficial acid onto the membrane was thoroughly wiped off with filter paper, and subsequently, it was used to prepare the MEA. The doped membrane was sandwiched between two electrodes, hot-pressing the whole system at 130 °C and 100 kg cm^{-2} for 15 min. Once the three MEAs were ready, they were inserted into the stack.

Cell hardware consisted of two bipolar (Quintech, Germnay) and two monopolar plates made of graphite (Sofacel, Spain), into which it was machined channels with four step serpentine channels geometry. Thus, 3 MEAs of 50 cm^2 each were assembled. Within the monopolar graphite plates, heating rods were fitted in order to heat the fuel cell up. During the measurements, the fuel cell was fed with pure hydrogen and oxygen or air, at different flows and stoichiometries, at atmospheric pressure and with backpressure up to 2 atm. Temperature was controlled with the aid of a temperature controller (CAL 3300, Cal Controls Ltd., UK) [8,15].

The polarisation curves were carried out as follows: firstly, the fuel cell was kept at constant temperature (125 °C) for 24 h, monitoring the cell voltage at a constant current density of 0.2 A cm^{-2}. Once fuel cell voltage was stable, cyclic voltammetries (CV) were carried out in order to characterize the stack, for this purpose was used a Power Station™ (Electrochem Inc., EE.UU). The CV was made at different oxygen flow rates and different oxygen and hydrogen stoichiometries at 125 °C. The performance was also measured at different cathode and anode back-pressures with constant fuel and comburent flow rates. The effect of temperature and the use of air as comburent were also evaluated. In order to know the durability and stability of the high temperature PEM fuel cell stack based on PBI, we operated at constant current (0.2 A cm^{-2}) over 185 h. During the stability test, every day the acid leach on both cathode and anode was measured and a series of dynamic loads were performed for developing response of the stack performance.

3. Results and discussion

3.1. Operation variables study

Fig. 1 shows performance results of the 150 cm^2 stack cell at different oxygen flow rates and 1500 ml min^{-1} of hydrogen flow rate. It is observed that the cell performance increased significantly from 554 ml min^{-1} to 1105 ml min^{-1} O_2 due to that at high currents, reagent requirements are much higher, according to Faraday's Law, than at low currents. Therefore, the stack performance drops at current density near 0.6 A cm^{-2} for an O_2 flow rate of 554 ml min^{-1}, due to the absence of reagent available to carry out the reaction.

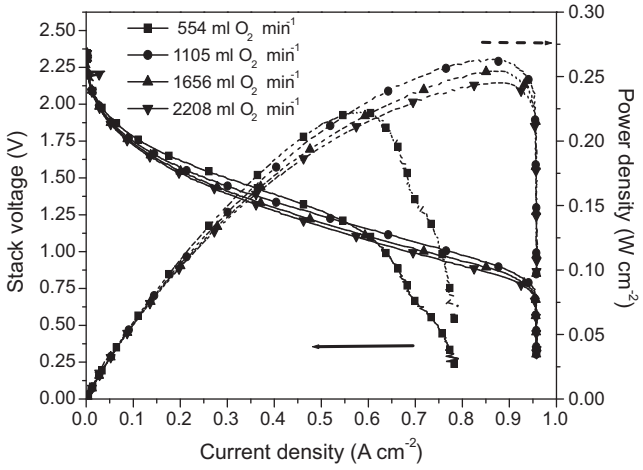

Fig. 1. Stack performance at different oxygen flow rates. H_2 = 1500 ml min^{-1}; T = 125 °C; P = 1 atm.

Values of O_2 flow rate higher than 1105 ml min^{-1} seem not increase the performance and even a decrease on the stack performance was observed. This could be due to that the excessive unreacted comburent could generate water vapour and phosphoric acid drags. Hence, the excessive comburent could cause membrane dehydration with the consequent ohmic drop at intermediate current densities. This ohmic drop is not observed when was increased the O_2 flow rate. It could be said that the different performances of the stack at high O_2 flow rates could be due to the experimental error.

Different tests were conducted at different pressures in both anode and cathode. The obtained results are shown in Fig. 2. The tests were carried out at constant reagent flow rates. Fig. 2a shows the effect of fixed O_2 back-pressure at 0.93, 1.43 and 1.93 atm and Fig. 2b shows the effect of fixed H_2 back-pressure at 0.93, 1.43 and 1.93 atm.

A higher back-pressure allows improved stack performance since the reactions are accelerated at both cathode and anode of the cell due to a partial pressure increase of the reactant gases. A higher voltage can be reached at a higher pressure, based on Nernst equation [16]. In Fig. 2, it can be seen that the open circuit voltage (OCV) and the limiting current density increase when the back-pressure increases. Moreover, it is also found that a back-pressure increment on the cathode (Fig. 2a) would cause a higher stack performance increase than on the anode (Fig. 2b). This is because such a pressure drop across the membrane results in a barrier for back diffusion, which takes place to keep the membrane hydrated [16].

Further information about the effect of the back-pressure can be found in Table 1, which shows how much the total power of the stack increase, when back-pressure was applied in cathode and anode. It is observed that the net power is higher when the pressure was increase 1 atm and it is only worthy increase the cathode which is the limiting electrode. On the one hand, as it was mentioned above, higher back-pressure lead to higher power out put. On the other hand, it was not observed a saturated point or negative effects beyond maximum operation back-pressure (1.93 atm) even small leaks were detected in the system at higher pressures. This is the reason why was not operated at higher back-pressure.

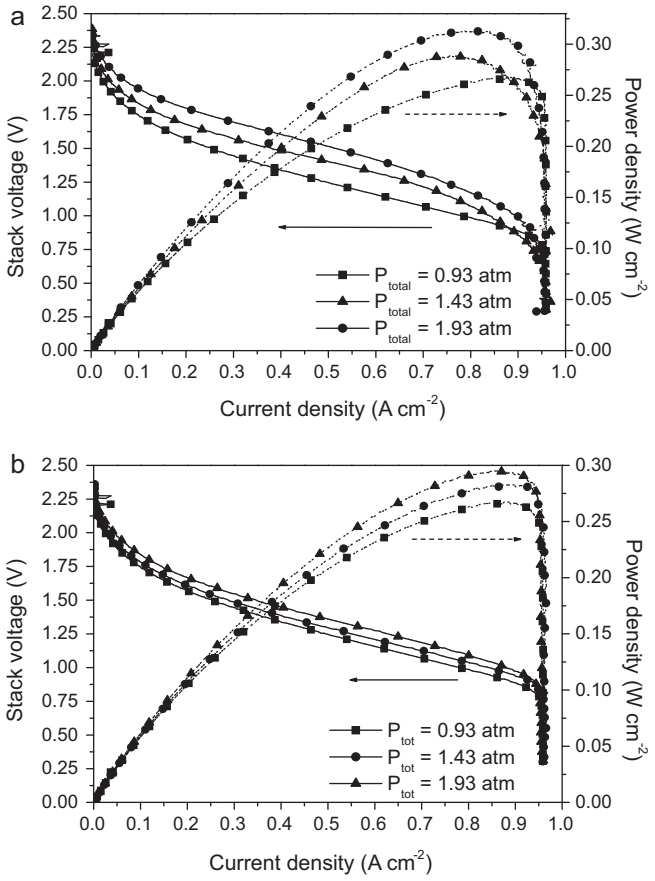

Fig. 2. Stack performance at different pressures. (a) Pressure effect on cathode and (b) pressure effect on anode. $T = 125\,^{\circ}C$; $H_2 = 1500\,ml\,min^{-1}$; $O_2 = 1105\,ml\,min^{-1}$.

The operation mode which provides a constant flow of reagents, does not allow to use them efficiently, since the combustion rate is not proportional to the reactive flow rate supplied, i.e., at low current densities a large excess of reagents is not consumed, resulting in excessive expenditure of reagents involved. Operating at constant stoichiometry (different reagents flow rate for different current densities) means to perform with a constant reagent excess and a better use of reactive can be achieved.

In order to minimize the use of reagents a series of test at different stoichiometries were made. Fig. 3 shows the stack performance at different oxygen stoichiometries (λ_{O_2}) and constant flow rate of hydrogen. From Fig. 3, it can be observed that using a stoichiometric amount of oxygen, which means $\lambda_{O_2} = 1$, major performance losses in the stack were obtained. At this stoichiometry, the flow of comburent placed on the stack is insufficient for very small current densities, about $0.15\,A\,cm^{-2}$, this means the existence of many active sites on the catalyst that are not being supplied with oxygen, due to the lack of this reagent in the system. For the stoichiometry of 1.5, lower performance losses than for the case of stoichiometry of 1 were obtained but still remain a loss of

Table 1
Stack power increased, power consumed and total power increased when backpressure is applied.

	ΔP (atm)	ΔW_{stack} (W)	$\Delta W_{consumed}$ (W)[a]	ΔW_{total} (W)
Anode	0.5	+1.95	−1.09	+0.86
	1	+3.9	−1.85	+2.05
Cathode	0.5	+3.6	−0.8	+2.8
	1	+7.35	−1.36	+5.99

[a] Power consumed to reach the backpressure in the stack by the device.

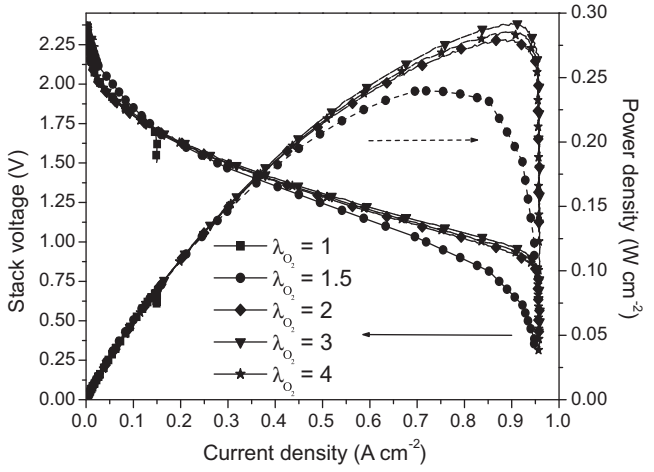

Fig. 3. Stack performance at different oxygen stoichiometries. $H_2 = 1500\,ml\,min^{-1}$; $T = 125\,^{\circ}C$; $P = 1$ atm.

performance compared to the rest of higher stoichiometries tested ($\lambda_{O_2} = 2$; $\lambda_{O_2} = 3$; $\lambda_{O_2} = 4$).

For the higher oxygen stoichiometries tested, the influence of the stoichiometry of the comburent has less influence compared to previously studied cases ($\lambda_{O_2} = 1$ and $\lambda_{O_2} = 1.5$). The difference between the maximum power peaks obtained for stoichiometries of 2, 3 and 4 represents an error of 4.3%, this could be due to experimental error. If the performance of the cell remains constant, it implies that the anode hydrogen is being completely consumed, while the cathode fuel is in excess [17]. Therefore, the use of a stoichiometry higher than two ($\lambda_{O_2} = 2$) does not produce enhancement of the fuel cell stack performance. Nevertheless, a $\lambda_{O_2} = 3$ was decided to use in the following experiments.

Once finished the test at constant oxygen stoichiometry, a two-week shut-down stage was performed in order to know how the effect in the fuel cell stack performance is. There was a significant performance loss in the stack as it is shown in Fig. 4. Fig. 4a shows the single cell performance before the two-weeks shut-down and Fig. 4b shows the single cell performance after the two-weeks shut-down. Each cell has been labelled from 1 to 3. The cell 1 was the inlet of the reagents and in the cell 3 the outlet. All the cells have the same inlet flow because there is a collector that distributes the reagents through each cell.

If Fig. 4a and b are compared, there are wide differences in the behaviour of the cell. In the case of the single cell 1, it can be observed that after the shut-down stage it was the cell that performed worse and there is a very sharp drop in performance reaching very low current densities. This behaviour can be explained only after serious damage occurred in the MEA during the shut-down stage, and this might be due to the deactivation of the catalyst or possible losses of the mechanical properties of the membrane due to a fracture of it [18,19].

The behaviour shown by cells 2 and 3 also differ markedly before and after the shut-down stage, both cells have high losses due to the deactivation of the catalyst and enhancement of the ohmic resistance after the stop. Also mass transfer problems appear at smaller currents densities. Therefore, the contribution of each of the losses leads to reduce the performance of each single cell and hence the global performance of the stack is reduced.

If the maximum peak powers, normalized to the Pt load in each cell of the stack (cell $1 = 0.64\,W\,mg\,Pt^{-1}$; cell $2 = 0.76\,W\,mg\,Pt^{-1}$; cell $3 = 0.73\,W\,mg\,Pt^{-1}$), and the results obtained by our group in a single cell with the same electrodes and dimensions [20] ($0.64\,W\,mg\,Pt^{-1}$) are compared, it can be observed that the peak powers were similar. Thus, the performance of the cells of the stack

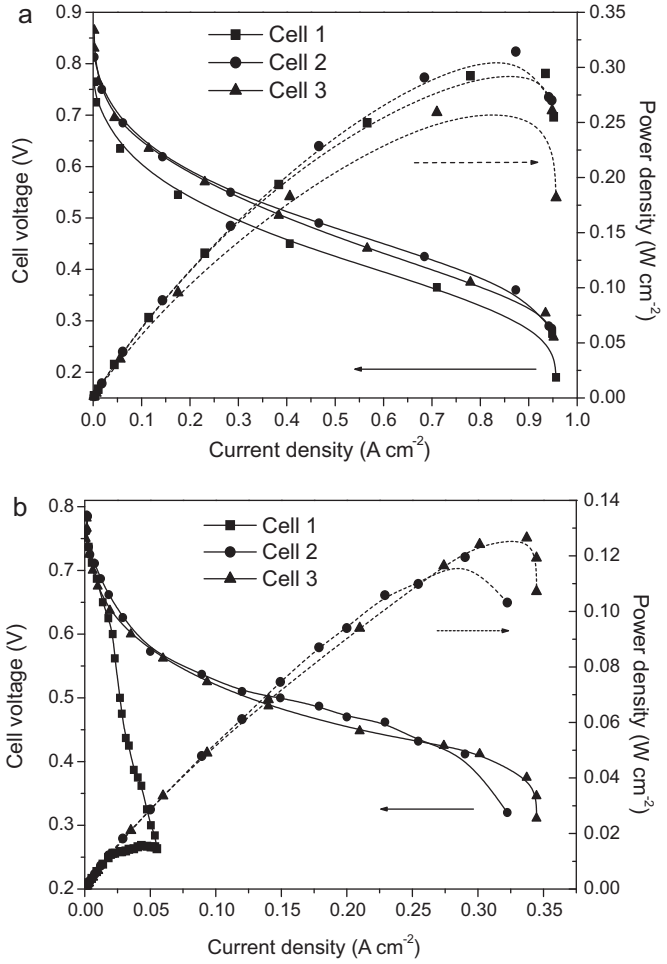

Fig. 4. Single cell performance (a) before and (b) after two-weeks shut-down. λ_{O_2} = 3; H_2 = 1500 ml min^{-1}; T = 125 °C; P = 1 atm.

is similar when they are running in single cell test with the same size, but if they are compared with the peak power (1 W mg Pt^{-1}) of a 5 cm^2 single cell with electrodes of the same composition [9], the yield is poorer when scaling-up. This could be due to mass transfer limitations in the larger electrodes. Thus, the peak power in the 5 cm^2 single cell was reached at 1.5 A cm^{-2} whereas the cells of the stack reached their maximum powers at 0.85 A cm^{-2} approximately.

The performance of a PEM fuel cell stack in the region where the activation losses govern can be represented by the Tafel equation (Eq. (1)):

$$E = E_{rev} + b \log i_0 - b \log i \quad (1)$$

where E, E_{rev}, b, i_0 and i are the electrode potential, reversible potential, Tafel slope, exchange current density and current density, respectively. Table 2 shows the Tafel slopes before and after the shut-down stage. As shown in Table 1, Tafel slopes increased after the stop of the stack at a constant temperature of 125 °C, higher Tafel slopes mean a decrease in the activity of the catalyst, which is attributed to its degradation during the two-weeks shut-down stage.

After the shut-down stage, the Tafel slope of cell 1 is twice higher than before shut-down stage. Nevertheless, the Tafel slope of cell 1 is not so high to explain the poor performance obtained after the shut-down. This indicates that the loss of the catalyst activity is not the only cause of the degradation. For the other single cells, the Tafel slopes increase less than in the case of the cell 1.

Table 2
Tafel slopes of the single cells operating at different operation conditions.

Cell	b (mV dec^{-1})			
	Before shut-down	After shut-down		
	O_2 T = 125 °C	O_2 T = 125 °C	Air T = 125 °C	Air T = 150 °C
1	66.9	126.1	130.2	110.6
2	88.2	102.4	108.3	85.4
3	64.3	89.3	98	77.7

According to Banham et al. [21], when Tafel slope changes from 60 to 120 mV dec^{-1} results on migration (ohmic) limitations in the porous catalytic layer which could explain our results.

The Tafel values before shut-down (shown in Table 2) of the different cells of the stack are very similar to those obtained in single cells (70.2 mV dec^{-1}) assembled by our group [9] with the same electrode composition but different size (5 cm^2). These values indicate that the electrochemical characteristics of our electrodes are similar independently of the size of the electrodes.

Although it has been reflected in the analysis of polarisation curves a power and a performance loss, it was decided to continue the completion of other experiments under these conditions, since the polarisation curves were repeated in each MEA and reproducibility was obtained therein (Table 2).

Moreover, the influence of hydrogen stoichiometry on the stack performance was evaluated. Fig. 5 shows the fuel cell stack performance at different hydrogen stoichiometries and a constant oxygen stoichiometry ($\lambda_{O_2} = 3$).

From Fig. 5, it can be seen that an adequate supply of fuel to the stack is very important for the proper operation of the system. The two lower hydrogen stoichiometries ($\lambda_{H_2} = 1.2$ and $\lambda_{H_2} = 1.5$) shown mass transfer problems at small current densities, about 0.06 A cm^{-2} and 0.21 A cm^{-2}, respectively, which means that the supplied fuel flow is not sufficient for current densities greater than those mentioned, with the consequent loss of performance in the fuel cell stack. It is also noted significant differences comparing the stoichiometries ($\lambda_{H_2} = 2.2$ and $\lambda_{H_2} = 2$). For a stoichiometry of $\lambda_{H_2} = 2.2$ there is a higher ohmic drop than for a stoichiometry of $\lambda_{H_2} = 2$. This ohmic loss could be due to the excess of unreacted fuel that could produce more dehydration process at the anode, since the anode works strictly at dry conditions [9]. This process leads to a conductivity loss of the electrolyte that worsens the proton conduction mechanism from

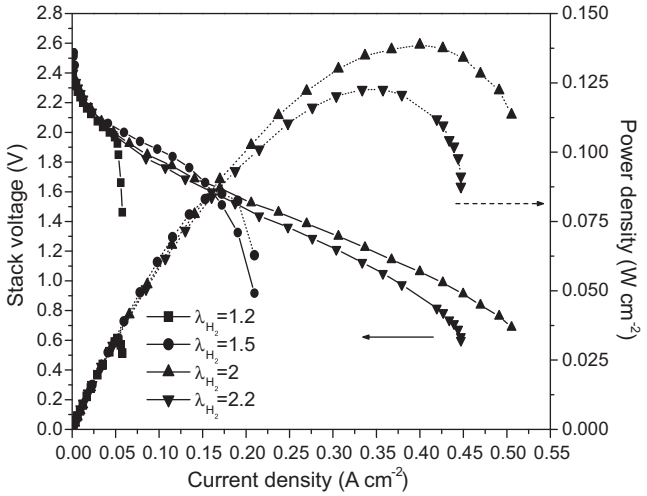

Fig. 5. Stack performance at different hydrogen stoichiometries. λ_{O_2} = 3; T = 125 °C; P = 1 atm.

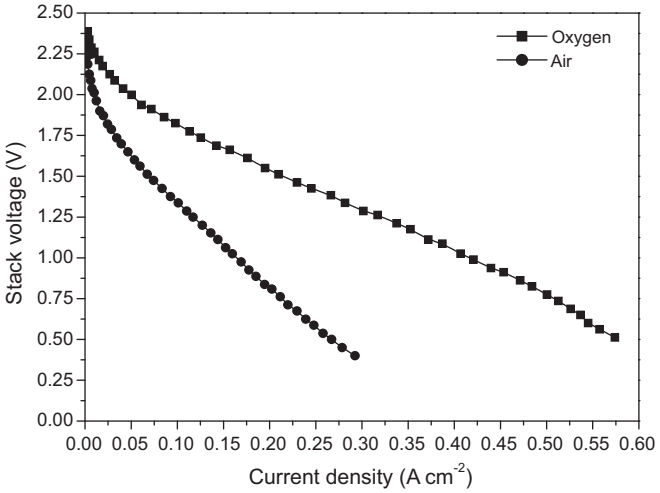

Fig. 6. Effect of replacing oxygen by air as comburent. $\lambda_{O_2} = \lambda_{O_2,air} = 3$; $\lambda_{H_2} = 2$; $T = 125\,^{\circ}C$; $P = 1$ atm.

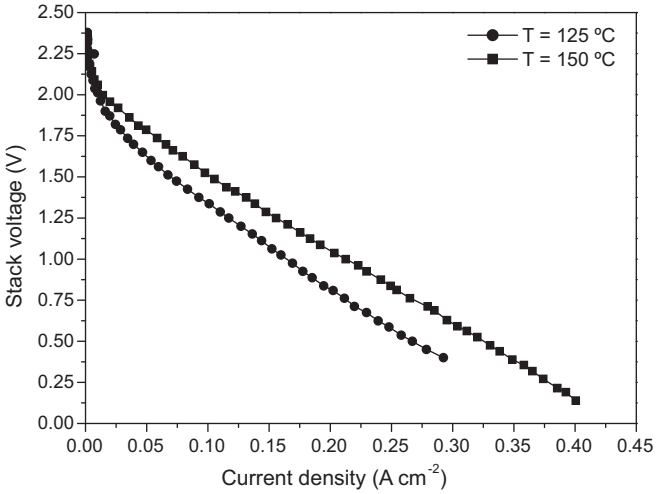

Fig. 7. Effect of temperature on fuel cell stack performance. $\lambda_{O_2} = \lambda_{O_2,air} = 3$; $\lambda_{H_2} = 2$; $P = 1$ atm.

the anode to the cathode, with the consequent loss of performance.

The effect of replacing oxygen by air was also studied. The fact for this change lies in the lower operating costs required for the stack. By providing atmospheric air instead of pure oxygen, the operating system is expected to be suitable for all applications (stationary and portable) with this type of technology [22]. Fig. 6 shows the polarisation curves of the stack running with oxygen and air under the same operation conditions. From Fig. 6, it can be seen a decrease in stack performance when using air as comburent. This fact is reflected in the Nernst's equation where the actual potential of the fuel cell decreases due to the O_2 partial pressure drop. In addition, the O_2 transport to the active sites of the catalyst finds higher diffusional resistance due to the presence of other gases that block the approach of O_2 to these active sites; therefore, part of the comburent does not react. The contribution of these resistances in the transport of oxygen to the catalyst active sites along with a decrease in the oxygen partial pressure as it is consumed in the stack, results in an increase of the concentration overpotentials by the fuel cell system [23].

In Table 2, it is also shown the Tafel slopes for both air and pure O_2 after the shut-down stage. It can be observed that the Tafel slopes are similar in both cases, which means that the reaction mechanism is almost independent on the O_2 concentration [24].

The last operation variable studied in this work was the effect of temperature. Increasing the cell performance is helpful to enhance electrochemical reaction rate and ionic transport in high temperature PEM, and accordingly the cell performance [9,17,25,26]. Fig. 7 shows the fuel cell stack performance at two different temperatures using air and hydrogen as reactive reagents.

It can be observed, in Fig. 7, an enhancement of the fuel cell stack performance when the temperature is increased from 125 °C to 150 °C as mentioned above. An increase on the operating temperature provides higher performance in the stack, in terms of voltage and current density. This is due to the improvement that occurs in the kinetic processes, mass transfer and the conductivity of the electrolyte [27,28] of each cell which provides an enhancement of the overall system performance. Thus, a temperature increase of 6% leads to an improvement of the stack voltage of 10% at 0.05 A cm^{-2}, 30% at 0.2 A cm^{-2} and 41% at 0.25 A cm^{-2}.

It is well known that in a high temperature PEMFC, the controlling electrode is the cathode (very slow reaction rate) [22,29,30]. An increase of temperature provides a higher oxygen reduction reaction rate; this means a marked improvement in the region of the polarisation curve dominated by activation losses. Also, in the ohmic region of the polarisation curve, it can be observed a decrease of the electrolyte resistance with temperature increase and also in the region of the polarisation curve where govern the concentration losses, it is observed an improvement in the stack performance. The mass transport problems are due to the limiting in the transport of reactant gases through the porous structure of the gas diffusion layer and the catalyst layer [31], due to the increase of temperature, mass transport is enhanced, increasing the limit current density of the fuel cell [16] and decreasing the mass transport problems.

As mentioned above, to operate at high temperature increases the activity of the catalyst. Table 2 also shows the different Tafel slopes for each cell, operating at a temperature of 125 °C and 150 °C using air as comburent. At a temperature of 150 °C, Tafel slopes were lower than those obtained at 125 °C, suggesting an increase in catalyst activity at higher temperatures. These results confirm that experimentally, the Tafel slope corresponding to the oxygen reduction reaction was found to increase with temperature in the low current density region [32,33].

3.2. Durability and stability test

Once all the above operation conditions were studied, a durability test was performed. The results obtained from a 185 h life test of the 3 cell stack operated with air, at 150 °C and a constant current density of 0.2 A cm^{-2} are shown in Fig. 8. Each 20 h approximately, the test was stopped and different measurements with dynamic load were carried out and also the leached acid in both cathode and anode were measured. These results are shown below.

Fig. 8 shows the variation of the stack voltage during the durability test. It can be observed a slight potential reduction of the stack in the first period of the test (24 h). Similar results were obtained by Zhang et al. in their preliminary study of their 6-cell PEMFC stack [34]. This may be due to a restoration of adequate humidity conditions in the system. When the system is stopped there is not reagent gas flux to drag the water vapour generated in the reaction, therefore, this water helps to improve the proton conduction mechanism of the electrolyte and thus the stack performance results in a higher potential in the early hours of the test and when the dynamic test were carried out [2] (shown in Fig. 8 with star symbol). Several researchers had reported long time life test of PBI based high temperature PEMFC [3,35–38] but not in stacks. Under a fixed loading current for a long time fuel cell test, two regions were observed in the output voltage versus testing time. The first

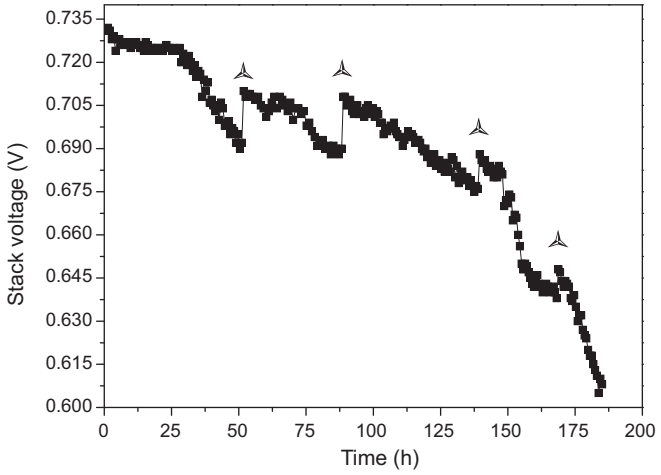

Fig. 8. Stability of fuel cell stack at a constant current of 0.2 A cm^{-2}. $\lambda_{O_2,\,air} = 3$; $\lambda_{H_2} = 2$; $T = 150\,^{\circ}C$; $P = 1$ atm.

initial testing period was the "activation region", in which cell voltage increased with operating time. Following this region was the "loss region", in which the cell voltage decreased with operating time. In the present work, the "activation region" did not appear due to that the stack was pre-activated during 24 h at 125 °C with a current density of 0.2 A cm^{-2} to carry out the experiments above described. The activation stage is a protocol that this group always makes before any measurement in order to ensure the stabilisation of the fuel cell performance [2,7–12,15]. As it is shown in Fig. 8, the overall effect of supply a constant load for long time causes potential losses. These results are comparable to those obtained by Wang and Chu [39]. These researchers demonstrated the operability of a single fuel cell at 150 °C for 200 h operation test using hydrogen and oxygen at 0.5 V of constant voltage. Also, it can be observed two different slopes where the voltage decreases. The first slope began at 28 h of operation and finished at 150 h approximately and the value of it was 0.27 μV s^{-1}, the second slope, where the voltage decreases dramatically, was from 150 h to 182 h and its value was 0.67 μV s^{-1}. The second slope was 2.5 times higher than the first slope.

Is have been proposed different degradation mechanisms to explain the voltage loss in a PEMFC. LaConti et al. [40] proposed a mechanism where the oxygen molecules permeate through the membrane from the cathode side and are reduced at the anode Pt catalyst to form hydrogen peroxide. H_2O_2 formation in oxygen reduction on Pt/C catalyst is greatly enhanced in the anode, where atomic hydrogen is adsorbed on Pt. The presence of H_2O_2 has been confirmed in the exhaust gas and directly in the membrane during operation of PEMFCs [19].

Other degradation mechanisms are the loss of catalyst active surface area by dissolution, due to the presence of phosphoric acid [41], the sintering of the catalyst [42], thermal stress in different parts of the stack, thermal degradation of the carbon support and corrosion of the carbon support due to the presence of the electrolyte [43]. The carbon corrosion produces electrical isolation between the catalytic particles and the carbon of the support, this support ensures the electrical contact between the bipolar plates. The electrical insulation decreases the electrochemical surface area available and produces a performance loss in the fuel cell [44,45].

Although these degradative events occur in the fuel cell, it is speculated that the phosphoric acid loss of the polybenzimidazole membrane is one of the main degradation mechanisms in this type of fuel cells [14]. Thus, in order to complete the durability study of the fuel cell stack at constant current density, the amount of phosphoric acid leached was measured. Fig. 9a shows the total amount of

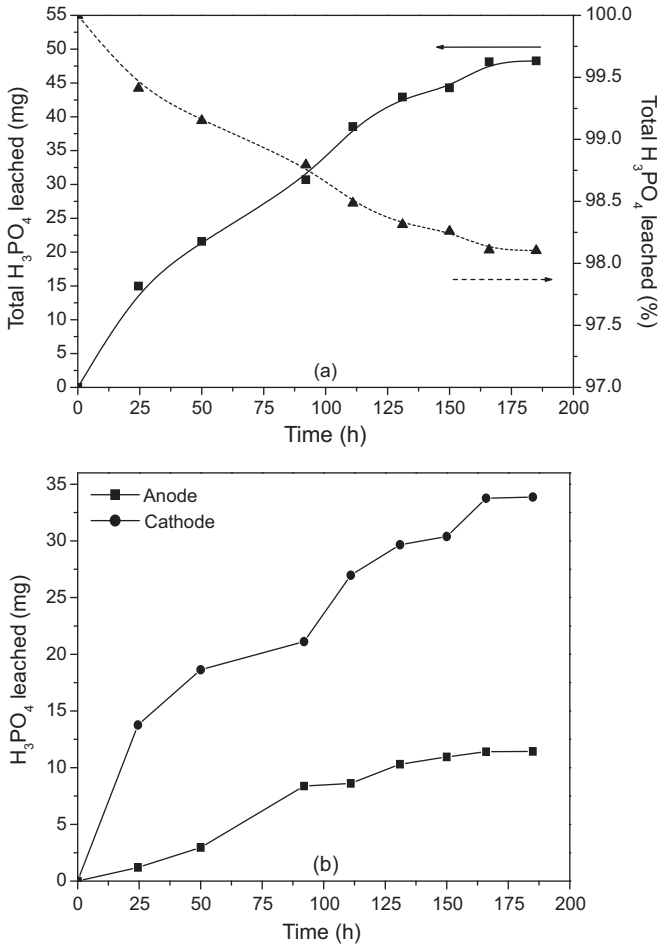

Fig. 9. Phosphoric acid leached from fuel cell stack during durability test at a constant current of 0.2 A cm^{-2}. (a) Total amount of H_3PO_4 leached; (b) amounts of H_3PO_4 leached from the cathode and the anode.

acid leached from the cell as milligrams and percentage and Fig. 9b shows the amount of acid leached from the cathode and the anode with time.

In Fig. 9a, it can be observed on the course of the operation time, a decrease in the slope and thus a decrease of the amount of phosphoric acid collected. One of the possible reasons of the higher acid leached at the beginning of the test is because during the manufacture of the MEA, where high pressure is applied, a certain amount of acid is distributed from the membrane to the gas diffusion layer (GDL) and remains in this layer where it is easier to be dragged by the reactant gases [14]. This phenomenon, together with the phosphoric acid which is used to impregnate the electrodes can be assumed to be the first quantities of electrolyte collected. Moreover, it can be seen that the amount of acid collected at the end of the test does not exceed 2% (w/w) of the total initial acid that contained the fuel cell stack.

It is difficult to associate the voltage drop of the fuel cell stack with electrolyte loss [14]. Different authors remain that the dissolution of Pt [46], Pt agglomeration [47] and corrosion of the carbon support [48,49] are the mechanisms that limit nowadays the operability of such technologies.

From Fig. 9b it can be observed that the acid leached from cathode is three times higher than the acid leached from the anode. This is because the water vapour generated in the reaction on the cathode side drags part of the phosphoric acid.

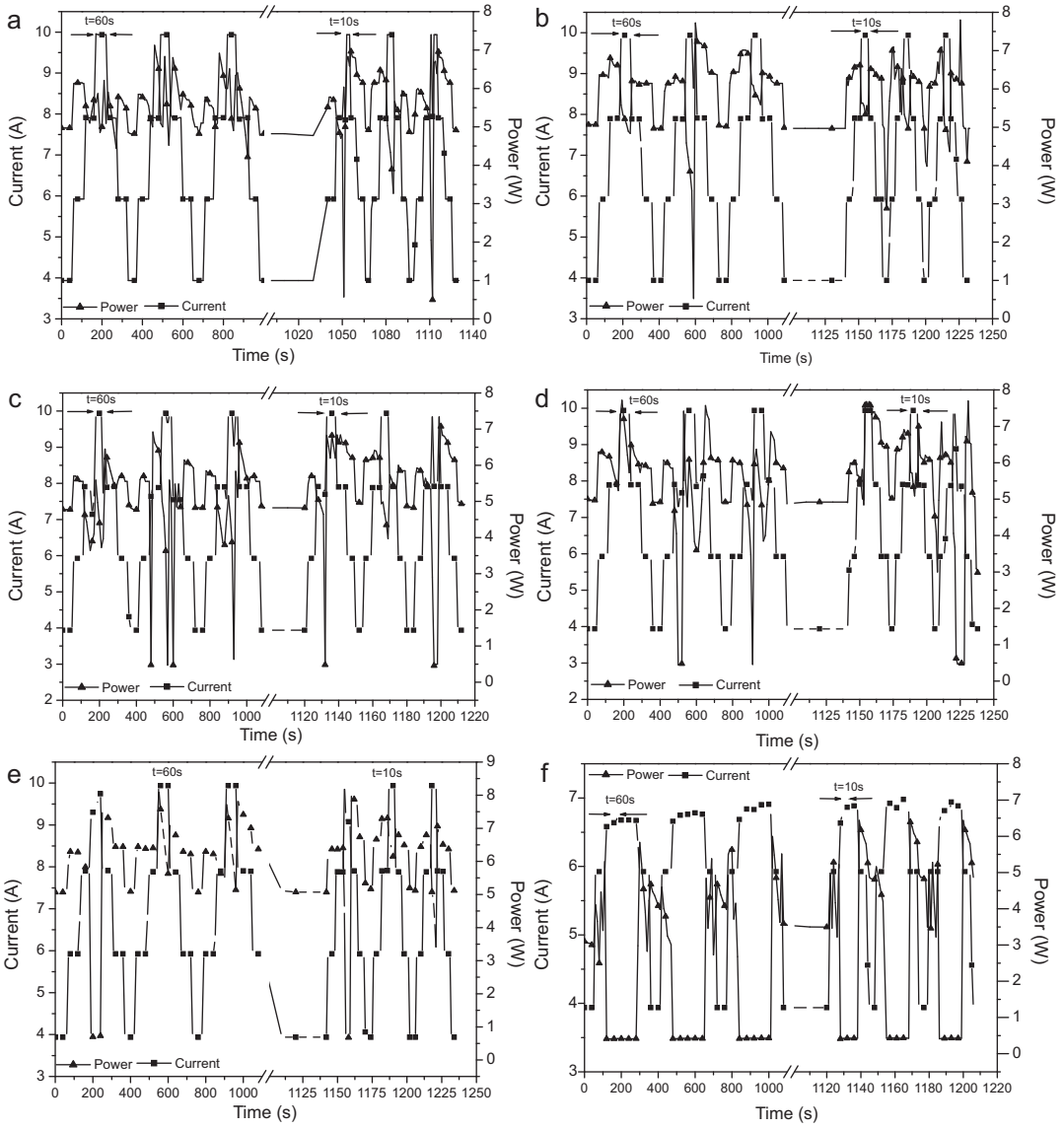

Fig. 10. Dynamic load response (a) after 40 h of operation; (b) after 68 h of operation; (c) after 96 h of operation; (d) after 124 h of operation; (e) after 152 h of operation and (f) after 185 h of operation. $\lambda_{O_2,\,air} = 3$; $\lambda_{H_2} = 2$; $T = 150\,^{\circ}C$; P = 1 atm.

3.3. Dynamic load test

As it has been said above, during the durability test, a dynamic load test was carried out at different times. The stoichiometry of the anode was $\lambda_{H_2} = 2$ and for the cathode was $\lambda_{O_2,\,air} = 3$. These dynamic load tests were conducted every 20 h, approximately. In this test, the fuel cell stack was subjected to different load regimes; this is to simulate the conditions in which this device would operate in transport applications. In order to simulate the acceleration, different step-constant current were applied and then different power generated. Each step is fixed with a current of 4, 6, 8 and 10 A for 60 s during three cycles and next three cycles the procedure was repeated for 10 s for a better understanding of the power generation of the stack. Changing the step-time allows to compare the effect of constant loading time on power generation. Fig. 10 shows the fuel cell stack response at different step-constant current loads cycles and at different times of operation.

It can be observed in Fig. 10a that for both step-times of 60 s and 10 s the current output response immediate. However, the generation of power output (for step-times of 60 s) is not observed high enough in the first cycle, but in the next two cycles it is observed a higher power output. Similar results were obtained by Weng et al. [50] on their 200 W PEM stack (not based on PBI) which concluded that higher current output generates the lower voltage and then apparently the power output is uncertain. It was observed that the total power output is similar for both step-times studied but it was obtained that the power output was moving onward for a step-time of 10 s. The same results were obtained for 68, 96, 124 and 152 h of operation (Fig. 10b–e). The results obtained in Fig 10f for an operation time of 185 h were something different. The current responds immediately but the higher current step range was not achieved and remains at 7 A. The power output also decreased and at the higher current range turns in lower values than at low current ranges. These results are due to that the fuel cell stack was seriously damaged as it was observed in Fig. 8, for 185 h of operation a great voltage decrease was reached.

4. Conclusions

From the study of the influence of stoichiometry of the reagent the values of $\lambda_{O_2} = 2$ and $\lambda_{H_2} = 2$ were the optimum under our

operation conditions. Moreover, for a better reagent utilization is recommended work at constant stoichiometry.

The back-pressure study showed an improvement of the stack performance being this more beneficial in the case of the cathode. As it was expected, an increase of temperature has a positive effect on the stack performance. Thus, an increase of 30% of the stack voltage at 0.2 A cm^{-2} was achieved when the temperature increased from 125 °C to 150 °C.

From the durability test it can be drawn that the stack suffered a progressive degradation till the 5th day. From this day, the degradation rate increased dramatically. The measurements of the acid leached showed that the acid losses were higher in the cathode than in the anode and the total acid loss was only a 2% on weight of the initial amount in the system (electrodes and membranes). Thus, the main degradation of the stack is not only due to the lack of electrolyte.

During the dynamic load analysis the stack gave an immediate response on the current and power output, only when the step-time is the shortest the power out-put was moved onward in time.

Finally, taking into account that the MEAs used in this work have been develop in our lab, with membranes and electrodes optimized from previous works [2,7–12,14], it has been demonstrated the feasibility of our MEAs in a stack. Although, further work is carrying out in order to improve these results, which are the first.

Acknowledgements

The authors want to thank the Ministry of Education and Science of the Spanish Government, the Junta de Comunidades de Castilla-La Mancha and the enterprise CLM-H_2 for the financial support through the projects CTM2007-60472 and PBI08-151-2045, respectively.

References

[1] S. Gottesfeld, T.A. Zawodzinski, in: R.C. Alkire, H. Gerischer, D.M. Kolby, C.W. Tobias (Eds.), Advances in Electrochemical Science and Engineering, vol. 5, Wiley-VCH, Weinheim, 1997, p. 195.
[2] J. Lobato, P. Cañizares, M.A. Rodrigo, J.J. Linares, J.A. Aguilar, J. Membr. Sci. 306 (2007) 47.
[3] H.L. Lin, Y.S. Hsieh, C.W. Chiu, T.L. Yu, L.C. Chen, J. Power Sources 193 (2009) 170.
[4] R.F. Savinell, M.H. Litt, US Patent 6,099,988 (2000).
[5] Q. Guo, P.N. Pintauro, H. Tang, S. OConnor, J. Membr. Sci. 154 (1999) 175.
[6] J.S. Wainright, J.-T. Wang, D. Weng, R.F. Savinell, M.H. Litt, J. Electrochem. Soc. 142 (1995) L121.
[7] J. Lobato, P. Cañizares, M.A. Rodrigo, J.J. Linares, G. Manjavacas, J. Membr. Sci. 280 (2006) 351.
[8] J. Lobato, P. Cañizares, M.A. Rodrigo, J.J. Linares, Electrochim. Acta 52 (2007) 3910.
[9] J. Lobato, P. Cañizares, M.A. Rodrigo, J.J. Linares, D. Ubeda, F.J. Pinar, Fuel Cells 10 (2010) 312.
[10] J. Lobato, P. Cañizares, M.A. Rodrigo, J.J. Linares, F.J. Pinar, Int. J. Hydrogen Energy 35 (2010) 1347.
[11] J. Lobato, M.A. Rodrigo, J.J. Linares, K. Scott, J. Power Sources 157 (2006) 284.
[12] J. Lobato, P. Cañizares, M.A. Rodrigo, D. Úbeda, J. Pinar, Linares J.J., Fuel Cells 10 (2010) 770.
[13] J. Lobato, P. Cañizares, M.A. Rodrigo, C. Ruiz-López, J.J. Linares, J. Appl. Electrochem. 38 (2008) 793.
[14] S. Yu, L. Xiao, B.C. Benicewicz, Fuel Cells 8 (2008) 165.
[15] J. Lobato, P. Cañizares, M.A. Rodrigo, J.J. Linares, C.-G. Piuleac, S. Curteanu, J. Power Sources 192 (2009) 190.
[16] S.-S. Hsieh, C.-L. Feng, C.-F. Huang, J. Power Sources 163 (2006) 440.
[17] W.-M. Yan, C.-Y. Chen, S.-C. Mei, C.-Y. Soong, F. Chen, J. Power Sources 162 (2006) 1157.
[18] M.L. Perry, T. Patterson, C. Reiser, ECS Trans. 3 (2006) 783.
[19] R. Borup, J. Meyers, B. Pivovar, Y.S. Kim, R. Mukundan, N. Garland, D. Myers, M. Wilson, F. Garzon, D. Wood, P. Zelenay, K. More, K. Stroh, T. Zawodzinski, J. Boncella, J.E. McGrath, M. Inaba, K. Miyatake, M. Hori, K. Ota, Z. Ogumi, S. Miyata, A. Nishikata, Z. Siroma, Y. Uchimoto, K. Yasuda, K. Kimijima, N. Iwashita, Chem. Rev. 107 (2007) 3904.
[20] J. Lobato, P. Cañizares, M.A. Rodrigo, J.J. Linares, F.J. Pinar, D. Ubeda, J. Power Sources 196 (2011) 4209.
[21] D.W. Banham, J.N. Soderberg, V.I. Birss, J. Phys. Chem. C 113 (2009) 10103.
[22] F. Barbir, PEM Fuel Cells: Theory and Practice, Elsevier Academic Press, New York, 2005.
[23] Q. Li, R. He, J.O. Jensen, N.J. Bjerrum, Fuel Cells 4 (2004) 147.
[24] J. Zhang, Y. Tang, C. Song, J. Zhang, J. Power Sources 172 (2007) 163.
[25] L.J. Bonville, H.R. Kunz, Y. Song, A. Mientek, M. Williams, A. Ching, J.M. Fenton, J. Power Sources 144 (2005) 107.
[26] Z. Qi, A. Kaufman, J. Power Sources 109 (2002) 469.
[27] R. He, Q. Li, A. Bach, J.O. Jensen, N.J. Bjerrum, J. Membr. Sci. 277 (2006) 38.
[28] Q. Li, H.A. Hjuler, N.J. Bjerrum, Electrochim. Acta 45 (2000) 4219.
[29] N.H. Jalani, M. Ramani, K. Ohlsson, S. Buelte, G. Pacifco, R. Pollard, R. Staudt, R. Datta, J. Power Sources 160 (2006) 1096.
[30] J. Wu, X.Z. Yuan, H. Wang, M. Blanco, J.J. Martin, J. Zhang, Int. J. Hydrogen Energy 33 (2008) 1735.
[31] C. Lim, C.Y. Wang, Electrochim. Acta 49 (2004) 4149.
[32] J. Zhang, Z. Xie, J. Zhang, Y. Tang, C. Song, T. Navessin, Z. Shi, D. Song, H. Wang, D.P. Wilkinson, Z.-S. Liu, S. Holdcroft, J. Power Sources 160 (2006) 872.
[33] A. Parthasarathy, S. Srinivasan, A.J. Appleby, C.R. Martin, J. Electrochem. Soc. 139 (1992) 2530.
[34] X. Zhang, D. Zheng, T. Wang, C. Chen, J. Cao, J. Yan, W. Wang, J. Liu, H. Liu, J. Tian, X. Li, H. Yang, B. Xia, J. Power Sources 166 (2007) 441.
[35] J. Hu, H. Zhang, Y. Zhai, G. Liu, B. Yi, Int. J. Hydrogen Energy 31 (2006) 1855.
[36] G. Liu, H. Zhang, J. Hu, Y. Zhai, D. Xu, Z.-G. Shao, J. Power Sources 162 (2006) 547.
[37] T.J. Schmidt, J. Baurmeister, J. Power Sources 176 (2008) 428.
[38] L. Xiao, H. Zhang, E. Scanlon, L.S. Ramanathan, E.-W. Choe, D. Rogers, T. Apple, B.C. Benicewicz, Chem. Mater. 17 (2005) 5328.
[39] C.-P. Wang, H.-S. Chu, J. Power Sources 159 (2006) 1025.
[40] A.B. LaConti, M. Hamdan, R.C. McDonald, in: W. Vielstich, H.A. Gasteiger (Eds.), Handbook of Fuel Cells – Fundamental, Technology and Applications, vol. 3, John Wiley & Sons, New York, 2003.
[41] Y. Zhai, H. Zhang, G. Liu, J. Hu, B. Yi, J. Electrochem. Soc. 154 (2007) B72.
[42] J. Hu, H. Zhang, Y. Zhai, G. Liu, J. Hu, B. Yi, Electrochim. Acta 52 (2006) 394.
[43] D.A. Stevens, J.R. Dahn, Carbon 43 (2005) 179.
[44] L.M. Roen, C.H. Paik, T.D. Jarvi, Electrochem. Solid-State Lett. 7 (2004) A19.
[45] K.H. Kangasniemi, D.A. Condit, T.D. Jarvi, J. Electrochem. Soc. 151 (2004) E125.
[46] J. Aragane, T. Murahashi, T. Odaka, J. Electrochem. Soc. 135 (1988) 844.
[47] A. Honji, T. Mori, K. Tamura, Y. Hishinuma, J. Electrochem. Soc. 135 (1988) 355.
[48] K. Kinoshita, J. Bett, Carbon 11 (1973) 237.
[49] K. Kinoshita, J.A.S. Bett, Carbon 12 (1974) 525.
[50] F.-B. Weng, B.-S. Jou, A. Su, S.H. Chan, P.-H. Chi, J. Power Sources 171 (2007) 179.